INT 196/99 September 1999

BOLOMETRY ON THE TCV TOKAMAK

Jan Mlynar, Ivo Furno, Bernard Joye,
and Arno Refke

Bolometry on the TCV Tokamak

Jan Mlynář, Ivo Furno, Bernard Joye, and Arno Refke

Centre de Recherches en Physique des Plasmas, Association EURATOM-Confédération Suisse, Ecole Polytechnique Fédérale de Lausanne, CH-1015 LAUSANNE, Switzerland

Abstract:

Two different bolometric systems are applied on the TCV tokamak. First, a group of metal foil bolometers is used, among others, for tomographic reconstruction of plasma energy loss. Second, recently developed AXUV photodiodes with broad and flat spectral sensitivity are under tests. Unlike the foil bolometers, the photodiodes are insensitive to neutral particle flow. Both the systems are described and compared within this work with special regard to the tomography application.

1. Introduction

At present tokamaks, bolometric systems represent a standard diagnostic tool aimed at measuring the total radiation emitted from the plasma, which is important for evaluation of the plasma energy balance. Individual bolometric sensors are usually arranged into arrays in pinhole camera configurations to allow for spatial resolution of the measured signal. In that case, supposing the plasma is optically thin for the measured radiation, the observed signals correspond to integrals over the lines-of-sight so that standard tomographic methods may be applied to get the cross-section of the plasma total radiation.

Most bolometers consist of elements designed to absorb all the incident energy, so that the energy flux can be determined from bolometers' temperature rise and their thermal capacity. Naturally, this kind of bolometers is sensitive not only to radiation energy loss, but also to energy loss via neutral particles' flow. The thin foil metal resistor bolometers, which are applied as a standard diagnostics system on the TCV tokamak, represent a miniaturized example of this category.

Semiconductor bolometers, i.e. photodiodes with broad spectral sensitivity, form another group of bolometers. They respond only to radiation and have better sensitivity and time resolution than the foil bolometers. Until recently, their application in plasma physics was avoided because of their insensivity to low energy photons. Progress in deposition technologies has nowadays allowed the manufacture of the AXUV photodiodes, which exhibit high efficiency down to very low photon energies. Two arrays of these detectors have been successfully tested on the TCV tokamak this year.

2. Metal Foil Bolometers

Miniaturized, low-noise, thin golden foil bolometers, which nowadays belong to the TCV standard diagnostic systems, were originally developed for the ASDEX tokamak [1]. The foil bolometer design is presented in Figs. 1 and 2. A several μm thick gold layer absorbs the plasma radiation. The subsequent temperature rise of the golden foil causes a linear increase of the resistance value in the kΩ range.

Next to each active bolometer there is one so called reference bolometer, identical in design, but completely shielded against the measured radiation. The two bolometer signals are subtracted by means of a bridge circuit; noise is efficiently suppressed thanks to this improvement. The detector operates in a 50 kHz AC excited bridge circuit. The foil bolometers' thermal inertia allow for temporal resolution of approx. 10 milliseconds, their spectral response is displayed in Fig. 4.

Sixteen arrays of these miniaturized bolometers, each with four elements, are installed in 5 pinhole cameras around a poloidal cross-section of the TCV tokamak vacuum vessel, see Fig. 3 a.

3. Tomographic Reconstruction

An elaborate computer tomography (CT) code was originally developed for the reconstruction of the TCV soft X-ray profile [2]. A modified version of the code has been applied for the CT reconstruction of the TCV foil bolometry measurements. Sufficient information for CT reconstructions with space resolution of approx. 5cm can be obtained thanks to the bolometers' setup geometry.

The CT application in bolometry allows, among others, the separation of the energy losses of the confined plasma from the losses which occur outside the plasma volume.

In the case of bolometry a standard pixels' method is appropriate for the CT reconstruction, as no symmetries can be expected. So far we use rectangular mesh of pixels which covers the whole vessel cross-section, see Fig. 3 b. The relation between the 64 lines of view and the mesh of 10x28 pixels can be simply described by a set of 64 equations:

$$f_i = \sum_{j=1}^{280} T_{ij} g_j \qquad (1)$$

The emission level g_j in individual pixels has to be retrieved from the signal level f_i. The inversion of the equation (1) including the treatment of the underdetermined and ill-conditioned problem is by default provided by the minimum Fisher regularization method in our CT code, see [2]. An illustrative CT reconstruction result is presented in Fig. 6 showing poloidal cross-section of energy losses in a TCV diverted plasma discharge[1] in which a transition from a low confinement (L-mode) to a high confinement (H-mode) regime occurs at *t=0.45 s*. Plasma last closed flux surface is in dotted line in Fig. 6, contours show the reconstructed radiation distribution. Thanks to considerably lower particle loss during H-mode the radiation from the divertor region disappears (the left bottom part of the vessel). Next, a period of large Edge Localized Modes (ELMs)[2] can be clearly seen in the reconstruction after *t=0.56 s* as the radiation from the divertor at the vessel bottom increases. The increase is due to significant plasma energy losses during large ELMs.

Already the early experience with the tomography reconstruction of the bolometric data showed serious problems on the level of the CT sensitivity and consistency. First attempts to improve the CT results were oriented towards its smoothing procedures, because unlike the soft X-ray data, the bolometric data have a considerable experimental error (approx. 3%) and additional error is generated in time deconvolution of the data which has to be done due to the heat capacity of the

1. In the divertor configuration, the last closed flux surface of the plasma is defined solely by the magnetic field, so that plasma-surface interactions take place only in the separated divertor region, see e.g. [3]. The same diverted discharge offered a good opportunity to examine also the new AXUV bolometric photodiodes and to compare the two systems, see the next section, Fig. 10 and Fig. 11.
2. ELM is an edge plasma instability which is responsible for bursts of particle and heat losses, see e.g. [3].

foils ($\tau \sim 100$ ms). Though considerable progress has been achieved thanks to the adaptation of the CT smoothing procedures, the performance of the bolometry data inversion is still below the level expected for the given CT reconstruction method.

We suppose that the perpetual problems are caused by the fact that one of the fundamental assumptions of CT reconstruction is impaired: the plasma is obviously not transparent for neutral particles, which are nevertheless detected by the foil bolometers. A considerable support for this supposition comes from the CT consistency check, in which signals f_i are compared to the line integrals of the reconstructed image $\Sigma T_{ij}\, g_j$, see Fig. 5. The figure shows clearly that those channels, which observe the plasma along long paths, yield lower signal than expected. Moreover, the difference is more pronounced for the top camera[1] (channels # 1..8) which observes the most active region through the plasma core and less for the bottom camera (channels # 57..64) which can observe it directly, see Fig. 3 a. This behavior proves that the plasma is not optically transparent for the analyzed signal.

At present the CT code is upgraded to make it more appropriate to the specific needs of bolometry, including a new option of shaped pixels. However, substantial improvement of the tomography results is possible only if the neutral particle influence on the signal is eliminated.

4. AXUV Photodiodes

The layout of a typical AXUV array of photodiodes is in Fig. 7. On TCV we use a similar array of 16 photodiodes, its installation into a pinhole camera is show in Fig. 8. At present, the test diagnostic system on the TCV tokamak consists of two pinhole cameras viewing the plasma from above and below at the same toroidal location, see Fig. 3 c. The spectral response of the photodiodes is presented in Fig. 9. Notice their striking efficiency down to very low energies, which was not attainable until recently. The AXUV photodiodes are insensitive to <500 eV neutral particles and have a very short time response (<0.5 μs). For more details on the AXUV photodiodes installation on the TCV tokamak see [4].

1. As a matter of fact the top camera channels had to be excluded from the CT reconstruction input because of their distinct inconsistency with the rest of input data.

Already the first campaign of experiments early this year showed a promising performance of the new bolometric photodiodes. An example of the performance of two individual photodiode channels is presented in Fig. 10 together with the plasma D_α emission and electron density evolution. Notice that we present here the same discharge as discussed in previous section, comp. Fig. 6. The L-H transition at *t=0.45 s* is clearly seen in the rapid increase of average electron density together with the reduction in the D_α emission. The increase of electron density is interrupted by several large ELMs, visible as spikes in the D_α emission and also easily in the photodiode signals in the expanded view at bottom right in Fig. 10. Notice the outstanding time resolution which could never be attained by foil bolometers.

For the same discharge, data from foil bolometers and AXUV photodiodes are compared in Fig. 11 for two pairs of channels which view the plasma along the same lines-of-sight. The time variation of three ratios of the detector signals demonstrate the differences in response of the two diagnostics. In L-mode, the power detected by the metal foil bolometers is significantly higher than that measured by the photodiodes, namely for the bottom foil bolometer (signal pair 3/2 in the figure). During H-mode, agreement between the foil bolometers and the photodiodes is considerably improved. For the pair 3/2, however, the outburst of the ELM activity leads again to a large increase in the ratio. The likely interpretation of this behavior is again in terms of neutral losses, to which only the foil bolometers are sensitive. Recycling of neutrals is generally higher in L-mode compared to H-mode, as indicated also by the D_α emission (comp. Fig. 10). Similarly, the ELM instability leads to a temporal increase in neutral recycling, which influences namely the region of the divertor. The hot plasma core prevents the upper foil bolometer from seeing the neutral particle exhaust localized in the divertor (see also the previous section).

Unfortunately the present sparse geometry of the photodiodes setup prevent the CT reconstruction of their data. This will be step by step improved in near TCV future. Following the above analysis, with a more extensive photodiodes' diagnostics it will be also possible to obtain a spatially resolved neutral atoms emission by combining the AXUV photodiodes data with the foil bolometers measurements. This idea has been already discussed in [5].

6. Conclusions

A set of 64 foil bolometers is installed as a standard diagnostic system on the TCV tokamak. Its data have been successfully used in CT reconstruction of the distribution of plasma power losses, though only with a limited performance.

A prototype bolometric system using AXUV photodiode arrays has been tested on the TCV. Their high temporal resolution allows detailed monitoring of fast phenomena, inaccessible to foil bolometric techniques. Moreover, the AXUV photodiodes are insensitive to neutral particles.

Both the tomography consistency tests and the comparison of AXUV signals with the foil bolometers data indicate clearly that the neutral particle flow cannot be neglected nor assumed to penetrate the plasma. Herefrom the limited performance of the present CT analyses in bolometry and consequently a great potential of the AXUV photodiodes for their application in the tomography.

Acknowledgment

This work was partly supported by the Swiss National Science Foundation.

References

[1] Mast, K.F. et al.: *A low noise highly integrated bolometer array for absolute measurement of VUV and soft X radiation*, Review of Scientific Instruments, Vol. 62, N. 3 (1991), 744 -750

[2] Anton, M. et al.: *X-ray tomography on the TCV tokamak*, Plasma Physics and Controlled Fusion, 38 (1996), 1849 - 1878

[3] Wesson, J.: *Tokamaks*. Clarendon Press, Oxford, 1997 (second edition)

[4] Furno, I. et al.: *Fast Bolometric Measurements on the TCV Tokamak*, accepted for publication in Review of Scientific Instruments; LRP 632/99, CRPP EPFL Lausanne, April 1999

[5] Boivin, R.L. et al.: *High resolution bolometry on the Alcator C-Mod tokamak*, Review of Scientific Instruments, Vol 70, N. 1 (1999), 260-264

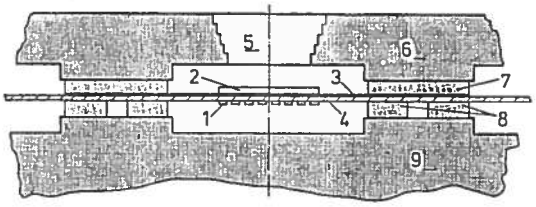

Fig.1 (top) Schematic design of the metal foil bolometer element

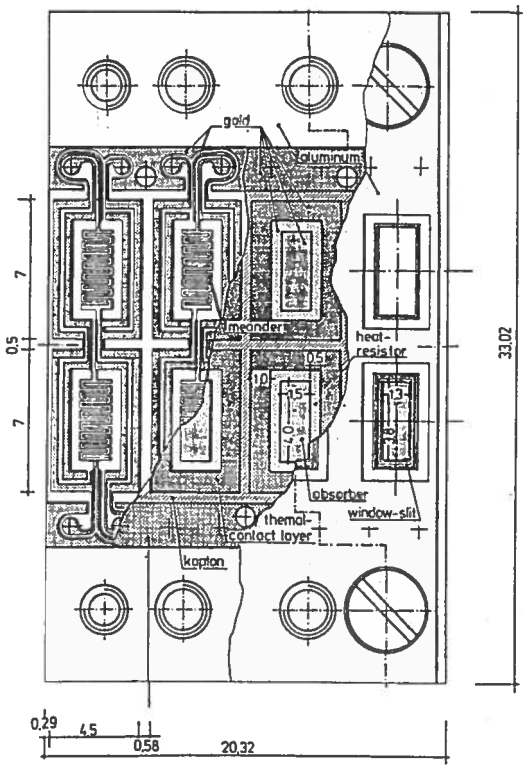

Fig.2 (right) Top view of the array of four metal foil bolometers. The upper blinded row of bolometers serves for reference.

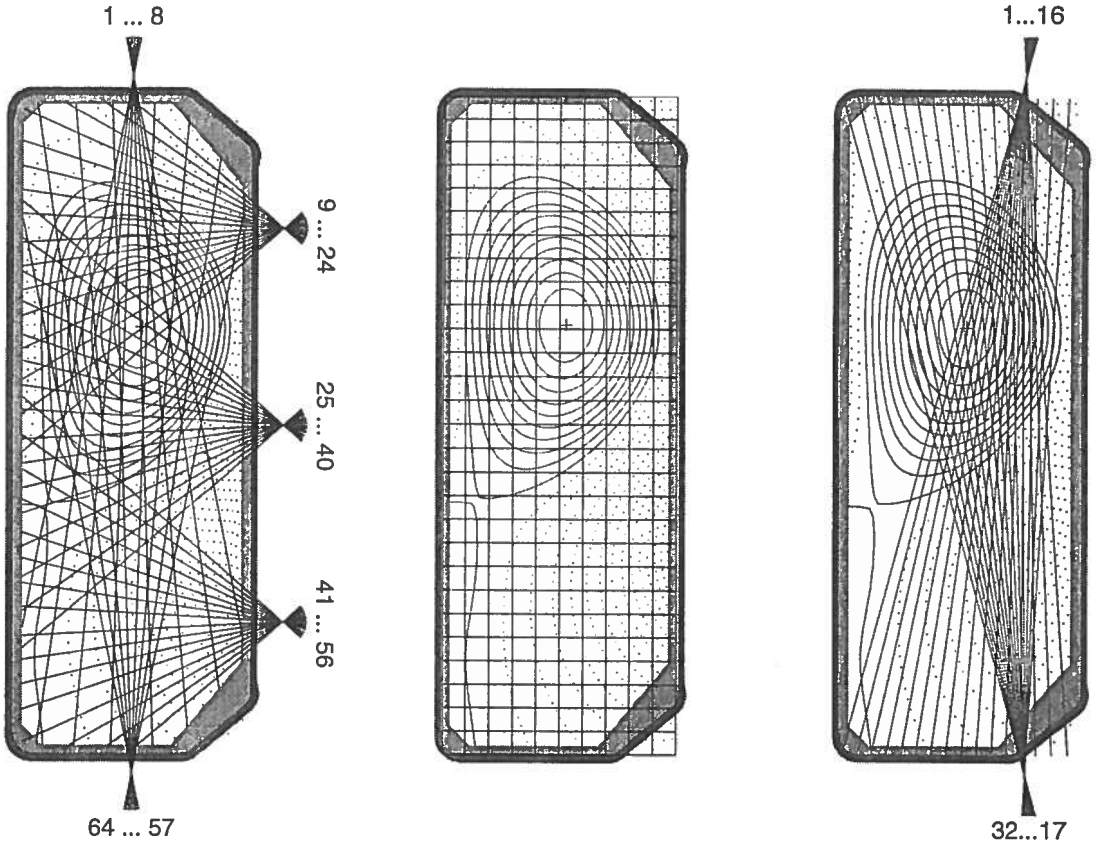

Fig. 3 The bolometry setup on the TCV tokamak (with contours of the plasma discharge #15539) a) setup of the foil bolometers, b) default pixels distribution for the CT reconstruction, c) setup of the AXUV photodiodes

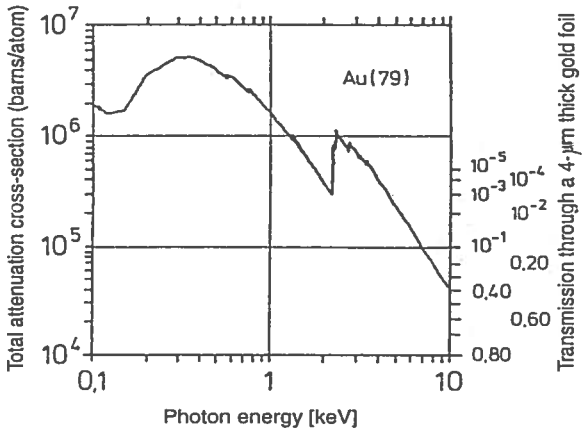

Fig. 4 Spectral response of the metal foil bolometers

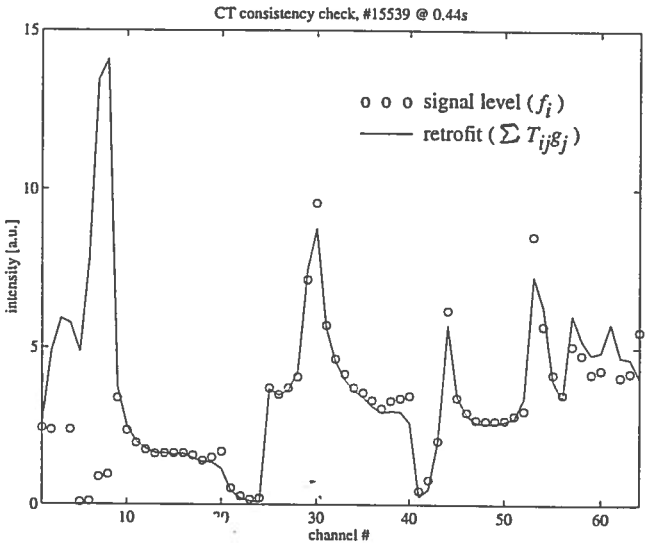

Fig. 5 A typical result of CT consistency check in bolometry

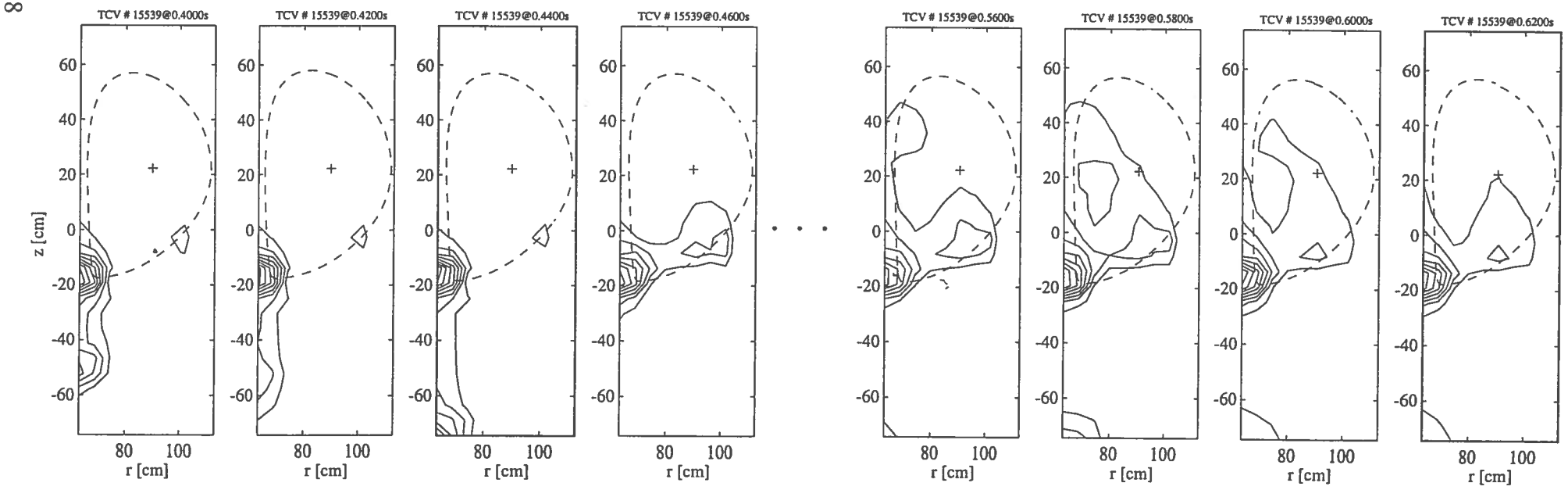

Fig. 6 CT reconstruction of foil bolometers data. Notice the influence of L-H transition at *t=0.45 s* and of large ELMs after *t=0.56 s*

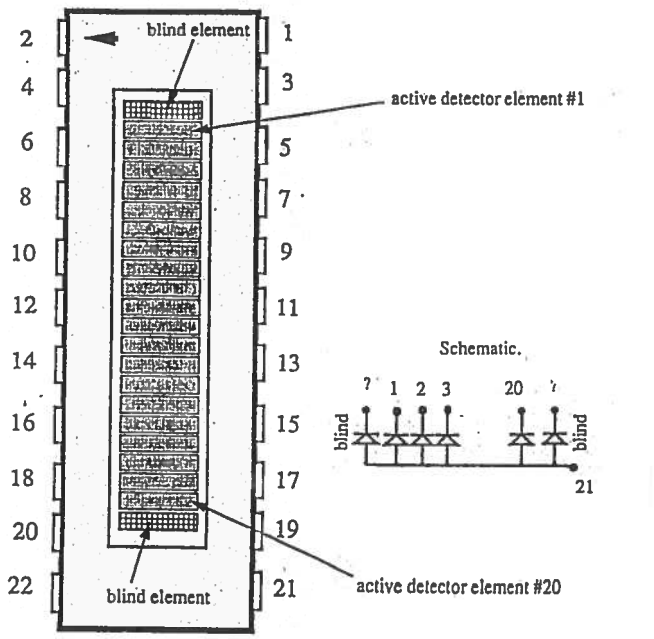

Fig. 7 The AXUV-20ELM array of photodiodes

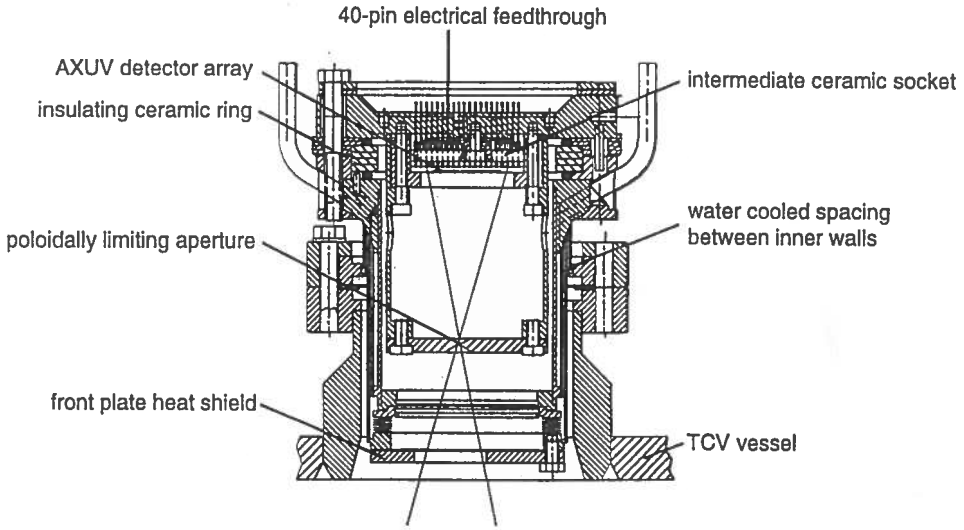

Fig. 8 Cross-section of the TCV pinhole camera for the AXUV array

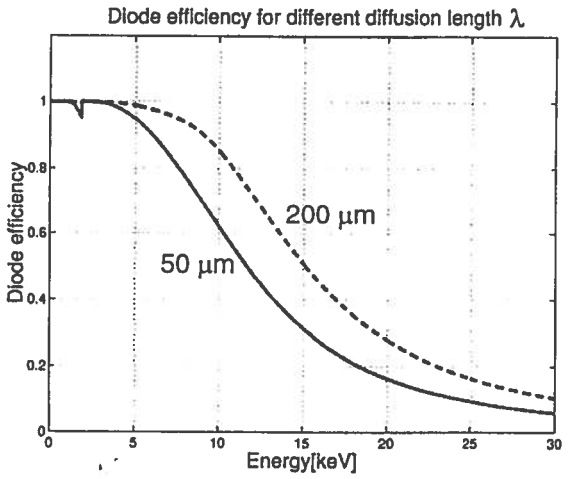

Fig. 9 Spectral response of the AXUV photodiodes (λ=50μm on TCV)

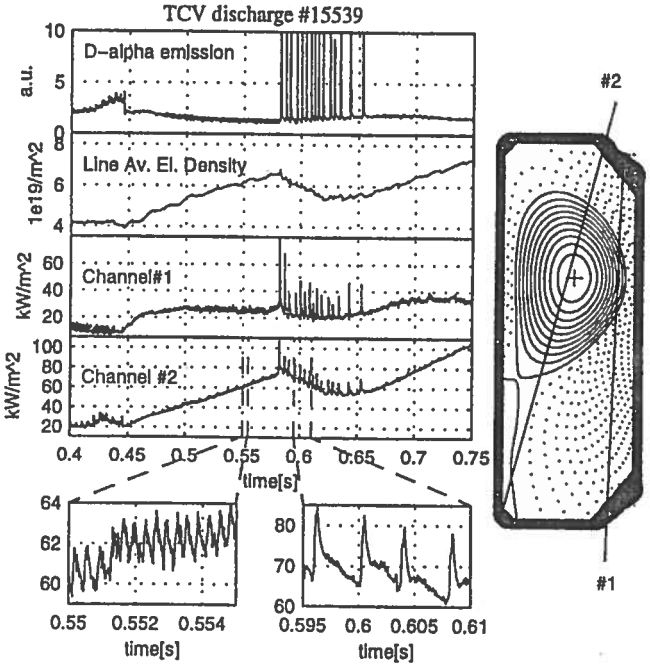

Fig. 10 An example of the AXUV photodiodes performance

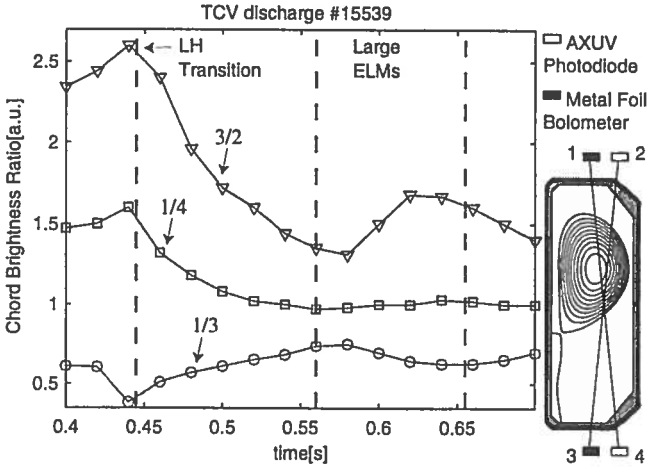

Fig. 11 Evolution of the foil bolometer / AXUV photodiodes signal ratio